

# Absolute negative resistance in tunnel junctions of nonequilibrium superconductors

M. E. Gershenzon and M. I. Faleĭ

*Institute of Radioengineering and Electronics, Academy of Sciences of the USSR*  
(Submitted 18 May 1987)

Zh. Eksp. Teor. Fiz. **94**, 303–314 (February 1988)

Absolute negative resistance (ANR) in superconducting tunnel junctions in which the electrode with the larger energy gap  $\Delta$  contains an excess of quasiparticles is studied experimentally. The quasiparticles were injected from an auxiliary tunnel junction. Absolute negative resistance was observed at low temperatures ( $\Delta/kT \gg 1$ ), for which the quasiparticle recombination time  $\tau_R$  is much longer. An independent determination of  $\tau_R$  shows that the Aronov-Spivak theory correctly describes both the range of parameters for which ANR is observed and the shape of the current-voltage characteristic. The results for  $\tau_R$  agree with theoretical calculations of the recombination time in disordered superconductors.

## 1. INTRODUCTION

Nonequilibrium processes in superconductors have been actively studied over the past 20 years. Because there are three distinct interacting subsystems (Cooper pairs, quasiparticle excitations, and phonons), the observed effects are highly diverse. Their study is important not only for basic research in the theory of superconductivity but also for practical applications. Tunnel junctions are widely used to study the energy gap and the quasiparticle distribution function in nonequilibrium superconductors excited by photons, phonons, and injected quasiparticles. In the latter case thin-film systems with two tunnel junctions are employed; one serves to generate the excess quasiparticle concentration in the common (injecting) electrode, while the other acts as a probe.<sup>1</sup> Figure 1 shows a typical experimental setup. The injecting tunnel junction is formed by the electrodes 1 and 3, the probe junction by electrodes 1 and 2. In what follows we will use subscripts to indicate the electrode to which a given parameter refers.

Experiments with double tunnel junctions can be arbitrarily divided into two groups: a) those in which one studies the stability of the superconducting state far from equilibrium, when the injection current is large ( $\delta\Delta/\Delta \sim 1$ , where  $\Delta$  is the order parameter at  $T = 0$ ); b) experiments at lower levels of quasiparticle injection ( $\delta\Delta/\Delta \ll 1$ ), in which one analyzes relaxation processes close to equilibrium. The experiments described below are of the second type, and we will be concerned only with this case in what follows. In most previous experiments of this type, the energy gap in the superconducting common electrode was less than in the second electrode ( $\Delta_1 < \Delta_2$ ). In this case it is easy to ensure that the second electrode is "transparent" to the excess phonons of energy  $\hbar\omega \approx 2\Delta_1 < 2\Delta_2$  generated by recombination of the nonequilibrium quasiparticles in the first electrode, simply by making it thinner than the mean free path  $\Lambda$  of these phonons in the second electrode. This circumstance greatly facilitates the interpretation of the experimental data since the second electrode may be assumed to be in equilibrium, and any change in the I-V characteristic of the probe junction is due to the excess quasiparticle concentration in the first electrode. On the other hand, for  $\Delta_1 < \Delta_2$  it is not possible to observe the Aronov-Spivak effect, which was predicted more than ten years ago<sup>2</sup> and is among the most striking

nonequilibrium effects in superconducting tunnel junctions.

As was shown in Ref. 2, under certain conditions the generation of an excess quasiparticle concentration  $\delta N_1$  in the electrode with the larger  $\Delta$  should cause the junction resistance at low bias voltages to become negative. This absolute negative resistance (ANR) is possible because in superconductors, the state density of the quasiparticles typically decreases with increasing quasiparticle energy. This is readily understood by using a "semiconductor" model for tunneling between superconductors (Fig. 2). For low temperatures  $\Delta_2/kT \gg 1$  and biases  $|V| < (\Delta_1 + \Delta_2)/e$ , most of the current is due to excess electron- and hole-like excitations tunneling out from the electrode with the larger  $\Delta$ . Because the quasiparticles tunneling against the applied junction voltage (quasi-hole excitations in Fig. 2) have a higher density of final states than do the excitations with quasiparticle charge of opposite sign, a net current flows opposite to the applied voltage, i.e., the absolute resistance is negative. We recall that in the equilibrium case, for  $T \neq 0$  the specific energy dependence of the state density in the superconductor determines the shape of the I-V characteristic for  $|V| = (\Delta_1 - \Delta_2)/e$  and the region of negative differential resistance for  $\Delta_1 - \Delta_2 < e|V| < \Delta_1 + \Delta_2$ .

In the present work we used two tunnel junctions with

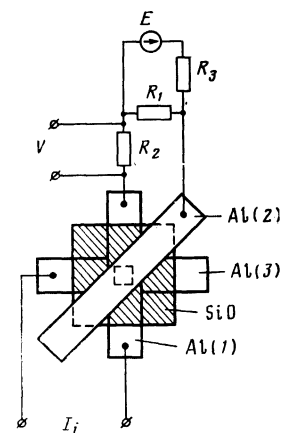


FIG. 1. Schematic of the experiment. The injecting tunnel junction is formed by the films Al(1) and Al(3), the probe tunnel junction by films Al(1) and Al(2). Typical resistor values were  $R_1 = 100 \Omega$ ,  $R_2 = 1-3 \Omega$ ,  $R_3 = 1-10^3 \Omega$ .

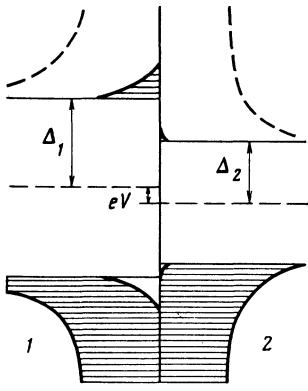


FIG. 2. "Semiconductor" model for tunneling between a superconductor 1, with an excess concentration of quasiparticles, and an equilibrium superconductor 2. The dashed curve shows the energy dependence of the density of states for quasielectrons.

$\Delta_1 > \Delta_2$  to analyze this effect experimentally. Reabsorption of excess phonons in the second electrode of the probe junction was avoided by making it thinner than the mean free path of the phonons with energy  $\hbar\omega \gtrsim 2\Delta_1$ . We note that for  $\Delta_1 > \Delta_2$ , in order to eliminate reabsorption of excess phonons in the second electrode the latter must be much thinner than if  $\Delta_2 > \Delta_1$  holds, because the mean free path for phonons with  $\hbar\omega > 2\Delta$  is considerably shorter than for phonons with  $\hbar\omega < 2\Delta$ . In addition to making the results simpler to interpret, the use of ultrathin electrodes also makes it easier to observe the ANR. The experimental observation of the ANR effect was reported in Ref. 3, where we studied tunnel structures on glass substrates; at the injection currents required to observe the ANR, the specimens were heated appreciably. In the present experiment we significantly extended the range of temperatures and injection currents for ANR by employing single-crystal sapphire substrates facilitating good thermal contact between the specimens and the thermostat. This enabled us to analyze the recombination of the excess quasiparticles in ultrathin superconducting films and to compare in detail the theoretical and experimental results regarding the shape of the I-V characteristic under ANR conditions and the parameter values for which ANR can be observed.

## 2. THEORY

Light-induced generation of excess quasiparticles was considered in Ref. 2, i.e., the photon energy was large compared to the gap ( $\hbar\omega \gg \Delta$ ). If the excess quasiparticles in the superconducting electrodes are assumed to relax to near-equilibrium distributions with chemical potentials  $\mu_i$  and temperature  $T$  equal to the thermostat temperature, we have the expression

$$I = \frac{\Delta_1(N_{1T} + \delta N_1)}{eR_N} \left\{ \left[ 1 - \exp\left(\frac{\mu_1 - \mu_2 + eV}{kT}\right) \right] \times \frac{\Delta_1 + eV}{[(\Delta_1 + eV)^2 - \Delta_2^2]^{1/2}} - \left[ 1 - \exp\left(\frac{\mu_1 - \mu_2 + eV}{kT}\right) \right] \frac{\Delta_1 - eV}{[(\Delta_1 - eV)^2 - \Delta_2^2]^{1/2}} \right\}, \quad (1)$$

for the quasiparticle current through the tunnel junction for arbitrary  $T$  and biases  $|V| \lesssim (\Delta_1 - \Delta_2)/e$ . Here  $R_N$  is the

junction resistance at supercritical temperatures,

$$\mu_i = kT \ln(1 + \delta N_i/N_{iT}), \quad N_{iT} = 2N(0)(2\pi kT\Delta_i)^{1/2} \exp(-\Delta_i/kT),$$

the  $N_{iT}$  are the equilibrium quasiparticle concentrations in the electrodes,  $\delta N_i$  the excess quasiparticle concentrations, and  $N(0)$  the single-spin density of states at the Fermi surface in the normal metal (we take it to be the same for the first and second electrodes). The condition for ANR at  $V = 0$  is<sup>2</sup>

$$\exp\left(\frac{\mu_1 - \mu_2}{kT}\right) - 1 > \frac{\Delta_1}{kT} \left[ \frac{\Delta_1^2}{\Delta_2^2} - 1 \right]. \quad (2)$$

We note that near the extrema on the I-V characteristic for  $|V| = (\Delta_1 - \Delta_2)/e$  ANR should occur when

$$\mu_1 - \mu_2 > \Delta_1 - \Delta_2. \quad (3)$$

For values  $(\Delta_1 - \Delta_2)/kT \lesssim 2.3$ , this condition is less restrictive than (2).

In our experiment the excess quasiparticle distribution was created by tunnel injection. At sufficiently low injection currents, for which the narrowing of the gap in the central electrode is small ( $\delta\Delta_1/\Delta_1 \ll 1$ ), the steady-state excess quasiparticle concentration can be found by solving the Rothwarf-Taylor equations<sup>4</sup>:

$$\delta N_i = [N_{iT}^2 + N_{iT}I_i\tau/ea_iS]^{1/2} - N_{iT}. \quad (4)$$

Here  $T_i/ea_iS$  is the quasiparticle source term in the middle electrode, of thickness  $a_i$ ;  $S$  is the area of the injecting junction, and  $\tau$  is the lifetime of the excess quasiparticles there. The time  $\tau$  depends on the recombination of the quasiparticles and the rate at which they escape from the central electrode by tunneling. In our experiment, the distance over which the excess quasiparticles diffused during the time  $\tau$  was much less than the linear dimensions of the injecting junction, so that escape by diffusion from the junction may be neglected. If recombination is the dominant process we have  $\tau = \tau_R(1 + \tau_{es}/\tau_B)$ , where  $\tau_R$  is the recombination time for the excess quasiparticles, and  $\tau_B$  and  $\tau_{es}$  are the lifetimes for phonons of energy  $\hbar\omega \approx 2\Delta_1$  corresponding to breakup of Cooper pairs and to escape from the central electrode, respectively.<sup>5</sup>

In the "pure" case  $q_{2\Delta}l \gg 1$ , where  $q_{2\Delta}$  is the wave vector for phonons with energy  $\hbar\omega = 2\Delta$  and  $l$  is the electron mean free path, the recombination time for quasiparticles with energy  $\varepsilon \approx \Delta$  is given by the expression<sup>5</sup>

$$\tau_R^{-1}(\Delta, T) = \pi^{1/2} \left(\frac{2\Delta}{kT_c}\right)^{3/2} \left(\frac{T}{T_c}\right)^{1/2} \exp\left(-\frac{\Delta}{kT}\right) \frac{1}{\tau_0}, \quad (5)$$

assuming  $\Delta/kT \gg 1$ . Here  $\tau_0 = 7\zeta(3)\tau_\varepsilon(0, T_c)$ , and  $\tau_\varepsilon(0, T_c)$  is the inelastic electron-phonon collision time, calculated at  $T = T_c$  and  $\varepsilon = 0$  for the case  $ql \gg 1$ . If the impurity scattering is pronounced, the electron-phonon interaction is modified and the expression for  $\tau_R$  ( $q_{2\Delta}l \ll 1$ ) becomes<sup>6</sup>

$$\tau_R^{-1}(\Delta, T) = 4 \left(\frac{2\Delta}{\pi kT_c}\right)^{1/2} \left(\frac{T}{T_c}\right)^{1/2} \exp\left(-\frac{\Delta}{kT}\right) \tau_\varepsilon^{-1}(0, T_c), \quad (6)$$

where  $\tau_\varepsilon(0, T_c)$  is the inelastic electron-phonon collision time for  $T = T_c$  in a "dirty" gas ( $ql \ll 1$ ) (Ref. 6):

$$\tau_\varepsilon^{-1}(T_c) = \frac{\beta}{5} \frac{k_F l}{(k_F u_i)^3} \left(\frac{\pi kT}{\hbar}\right)^4 \left[ 1 + \frac{3}{2} \left(\frac{u_i}{u_i}\right)^2 \right]. \quad (7)$$

Here the parameter  $\beta$  is  $\sim 0.7$  for aluminum (see Ref. 6 for more information),  $k_F$  is the Fermi wave vector, and  $u_l$  and  $u_t$  are the longitudinal and transverse phonon propagation velocities.

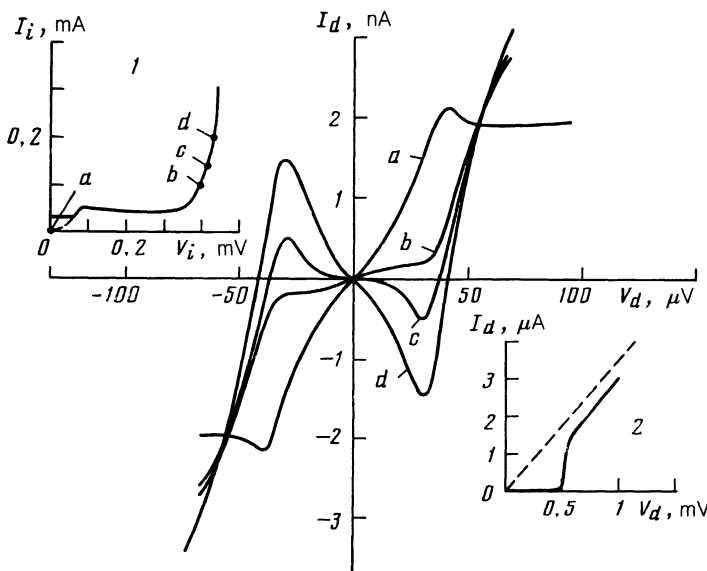
### 3. MEASUREMENT TECHNIQUE

The tunnel junctions were fabricated between aluminum films deposited by thermal vaporization on sapphire and glass substrates. The tunnel oxide was grown by exposing the films to air for 1–30 min. The injecting junction, of area 1 mm<sup>2</sup>, was formed by two films Al(1) and Al(3); above the critical temperature its resistance was 0.01–1 ohm. The area of the probe junction was determined by the area of the “window” in the SiO layer separating the films Al(1) and Al(2). The window was fabricated by successively sputtering two SiO layers of thickness  $\sim 30$  Å through masks rotated by 90° with respect to one another (the masks were strips  $\sim 0.3$  mm wide). These SiO layers evidently made the probe junction much less transparent than the injecting junction—the probe junction resistance (30–1000 ohm) was  $10^3$ – $10^4$  times larger than the resistance of the injecting electrode. The desired ratio  $\Delta_1/\Delta_2$  for the probe junction electrodes was achieved by choosing the thickness and degree of disorder of the aluminum films: their critical temperature was sensitive to the resistivity  $\rho$ , increasing from  $\approx 1.2$  to  $\approx 2.2$  K as  $\rho$  increased from  $10^{-6}$  to  $10^{-4}$  ohm·cm (see, e.g., Ref. 7). In most cases the middle electrode [Al(1) film] was sputtered at a rate of 2 Å/s; the partial oxygen pressure was  $P_{O_2} = (8-10) \cdot 10^{-5}$  mbar, and the thickness of the electrode was  $a_1 = 40-60$  Å. The film resistivity was  $\rho = (0.5-2) \cdot 10^{-4}$  ohm·cm, and the critical temperature was  $T_{c1} = 2.0-2.2$  K. The Al(2) and Al(3) films were sputtered at 5 Å/s and their thickness was  $a_2 = a_3 = 100-150$  Å; depending on the residual pressure during sputtering, their critical temperatures varied from 1.4 to 1.9 K. The relative difference  $(\Delta_1 - \Delta_2)/\Delta_1$  for our specimens was 0.05–0.3. Most of the data presented below were obtained for a specimen on sapphire with the following properties:

$$a_1 = 60 \text{ \AA}; T_{c1} = 2.15 \text{ K}; l_1 = 7 \text{ \AA}; a_2 = a_3 = 120 \text{ \AA};$$

$$T_{c2} = 1.86 \text{ K}; T_{c3} = 1.55 \text{ K}; \Delta_1 = 0.31 \text{ meV}; \Delta_2 = 0.27 \text{ meV}$$

$$R_N(\text{PTJ}) = 270 \text{ ohm}; R_N(\text{ITJ}) = 0.013 \text{ ohm}.$$



The bulk of the measurements were made for  $T$  between 0.4 and 1 K with the junctions immersed in liquid <sup>3</sup>He. A current source was employed to record the equilibrium I-V characteristics for the probe and injecting junctions, and a voltage divider (Fig. 1) was used to analyze how the excess quasiparticle concentration altered the I-V characteristic of the probe junction. The formulas

$$V_d = ER_1/(R_1 + R_3) - V, \quad I_d = V/R_2$$

were used to calculate the voltage  $V_d$  applied to the probe junction and the current  $I_d$  through it for  $|V_d| < (\Delta_1 + \Delta_2)/e$  and  $T < 0.8$  K. Here  $E$  is the emf of the source, and the above formulas were derived under the assumption that the current has a value  $\sim 10$  μA through the resistor  $R_1$  is much larger than the current ( $\leq 10$  nA) through the specimen.

### 4. EXPERIMENTAL RESULTS AND DISCUSSION

In the absence of an injection current, the I-V characteristics for all of the probe junctions are adequately described by the theory of one-electron tunneling between superconductors (see, e.g., Ref. 8), provided one allows for the effects of structural inhomogeneities and external noise, which tend to broaden the extrema on the I-V curves at  $|V_d| = (\Delta_1 \pm \Delta_2)/e$ . In particular, for specimens with nearly equal energy gaps  $[(\Delta_1 - \Delta_2)/\Delta_1 \ll 1]$ , the currents  $I_d^{\text{pl}}$  on the current plateau of the characteristic observed for  $\Delta_1 - \Delta_2 \lesssim e|V_d| \lesssim \Delta_1 + \Delta_2$  are accurately described by the expression<sup>1</sup>

$$I_d^{\text{pl}}(T) = [N_{1T}(T) + N_{2T}(T)]/4N(0)eR_N, \quad (8)$$

which is valid at sufficiently low temperatures.

Figure 3 shows how the I-V characteristic of the probe junction changes in response to an injection current  $I_i$ . As  $I_i$  increases,  $I_d$  is observed to drop for bias voltages  $V_d$  constant in the interval  $|V_d| \lesssim (\Delta_1 - \Delta_2)/e$ , while for  $|V_d| > (\Delta_1 - \Delta_2)/e$  the values  $I_d^{\text{pl}}$  corresponding to the current plateau increase (see the insert to Fig. 4). Reversing the sign of the injection current has no effect on the shape of the I-V characteristics, which remain symmetric about the coordinate origin. A region corresponding to absolute negative resistance appears on the I-V characteristic at a certain value  $I_i(T)$ : the current flows opposite to the voltage applied to

FIG. 3. Current-voltage characteristics for the probe tunnel junction, recorded at  $T = 0.52$  K for several injection currents: a)  $I_i = 0$ ; b) 0.1 mA; c) 0.14 mA; d) 0.2 mA. Insert 1 shows the I-V characteristic for the injecting junction at  $T = 0.52$  K, insert 2 the I-V characteristic for the probe junction at higher voltages  $V_d$ .

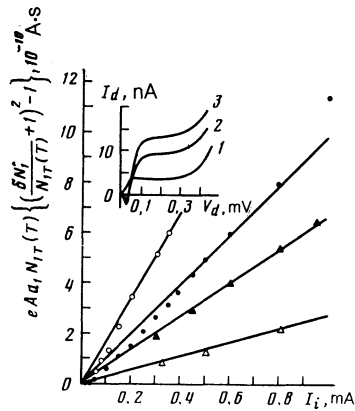


FIG. 4. Excess quasiparticle concentration  $\delta N_1$  in the film Al(1) as a function of the injection current for  $T = 0.74$  ( $\Delta$ ),  $0.63$  ( $\blacktriangle$ ),  $0.59$  ( $\bullet$ ), and  $0.54$  K ( $\circ$ ). The insert shows the I-V characteristics for the probe junction near the current plateau for  $T = 0.59$  K and  $I_i = 0$  (1),  $0.5$  (2), and  $1.0$  mA (3). The midpoint of the plateau ( $V_d = 0.2$  mV) was used in calculating  $\delta N_1$ , by Eq. (8).

the probe junction. Experiments carried out under conditions when the extrema at  $|V_d| = (\Delta_1 - \Delta_2)/e$  ( $I_i = 0$ ) were pronounced show that for our specimen, ANR sets in at  $|V_d| \approx (\Delta_1 - \Delta_2)/e$ . The ANR spreads throughout the interval  $|V_d| \lesssim (\Delta_1 - \Delta_2)/e$  as  $I_i$  increases; finally, when  $I_i = I_i^*$  the differential conductivity ( $G_0 = dI_d/dV_d = 0$ ) of the probe junction changes sign. The values  $I_i^*$  are strongly temperature-dependent and decrease rapidly with cooling; at a fixed temperature  $I_i^*$  increases with  $(\Delta_1 - \Delta_2)/\Delta_1$ , the difference between the energy gaps in the probe junction electrode. As  $I_i$  increases further ( $I_i > I_i^*$ ),  $|G_0|$  continues to increase until power dissipation in the injecting tunnel junction results in significant heating, or until the injection current exceeds the critical current for the superconducting film Al(1) and the latter is quenched.

For specimens on sapphire, the range of injection currents for which ANR was observed was bounded from above by the critical current for quenching of the electrodes in the injecting junction. For  $T \ll T_{c1}$ , the critical currents for our ultrathin Al films (of width  $\sim 1$  mm and thickness  $60 \text{ \AA}$ ) were typically  $2\text{--}3$  mA, in satisfactory agreement with estimates for the critical depairing currents for the case of a nonuniform current distribution over the cross section of a film of width  $W \gg \delta_1(T)$ , where  $\delta_1(T)$  is the effective penetration depth of the magnetic field into the thin superconducting film (see, e.g., Ref. 9). Due to their good thermal contact with the thermostat, the films on the sapphire substrates were not appreciably heated for  $I_i$  below  $1$  mA. The differential conductivity  $|G_0|$  therefore stopped increasing at currents  $I_i$  comparable to the critical current for the electrodes. For the specimens on glass, heating became important at much lower currents  $I_i$ : even for  $I_i \sim 0.1$  mA the dependence  $I_d^p(I_i)$  was exponential, indicating that the specimens were heated<sup>11</sup> (see below). In this case, ANR was observed in a much narrower range of currents  $I_i$ . For example, for the specimen on glass discussed in Ref. 3, the ANR disappeared when  $I_i \gtrsim 0.3$  mA. [We note that in these experiments the voltage applied to the injecting junction was always  $\sim (\Delta_1 + \Delta_2)/e$ , see Fig. 3, and the power evolved in the junction was essentially independent of the junction resistance in the normal state.]

Before the theoretical estimates can be compared with the experimental results for the magnitude of the ANR and the parameter values for which it is observed, one must know the lifetime of the excess quasiparticles in the central electrode [see expressions (1), (2), (4)]. In analyzing the experimental data we will thus start by considering the dependence of  $I_d^p$  on the injection current; this dependence provides an independent method of finding  $\tau$  (see, e.g., Ref. 11). Armed with a knowledge of  $I_d^p(I_i)$ , we can use Eq. (8) to estimate the excess quasiparticle concentration  $N_1(T)$  in film Al(1) under the assumption that the quasiparticle distribution in film Al(2) remains in equilibrium ( $N_2(T) \equiv N_{2T}$ ). This assumption is valid for our specimens. Indeed, excess phonons which are generated in the first electrode through the recombination of quasiparticles and which have energy  $\hbar\omega \approx 2\Delta_1 > 2\Delta_2$  are the only possible source of excess quasiparticles in the second electrode. [Under the experimental conditions, the current through the probe junction was  $1\text{--}10$  nA for  $|V_d| < (\Delta_1 + \Delta_2)/e$ ; the number of quasiparticles injected into the second electrode was consequently negligible.] The time required for the excess phonons to escape from the film Al(2) immersed in liquid  $^3\text{He}$  is given by<sup>12</sup>

$$\tau_{es} = 4a_2/\eta u \approx 2 \cdot 10^{-11} \text{ s}. \quad (9)$$

Here  $u$  is the speed of sound in the film and  $\eta = 0.2\text{--}0.5$  is the probability for transmission of a phonon across the film/liquid  $^3\text{He}$  interface.<sup>12</sup> For our ultrathin films, this time is much shorter than the lifetime  $\tau_B$  of the excess phonons determined by the breakup of Cooper pairs. [In aluminum films  $\tau_B = (1\text{--}2) \cdot 10^{-10}$  s (Ref. 15) for phonons of energy  $\hbar\omega \approx 2\Delta_1$  for  $T \lesssim 0.5T_c$ .] Because  $\tau_{es} \ll \tau_B$ , we may assume that the excess quasiparticle concentration in film Al(2) is much less than in film Al(1) ( $\delta N_2 \ll \delta N_1$ ) and, moreover, that phonon reabsorption does not influence the excess quasiparticle lifetime in the film Al(1).

Figure 4 plots  $\delta N_1(I_i)$  given by (8) for several temperatures; we see that there is a wide range of  $I_i$  for which the curves are well approximated by the solutions of the Rothwarf-Taylor equations corresponding to different values of  $\tau(T)$ . In the coordinates used in Fig. 4, Eq. (4) gives a straight line passing through the origin. The injecting junction for this specimen was a Josephson junction with critical current  $I_c = 0.035$  mA, hence there was no injection of quasiparticles for  $I_i < I_c$  in this case. This explains the nonlinearity of the experimental curves for  $I_i \lesssim 0.1$  mA. The abrupt increase in  $\delta N_1$  for  $I_i \gtrsim 1$  mA is due to bulk heating of the junction by the current flowing in the injecting tunnel junction. The absolute values  $\tau(T)$  can be deduced by comparing the theoretical and experimental curves  $\delta N_1(I_i)$  at various temperatures. For all of the specimens investigated,  $\tau$  depended strongly on temperature in the interval  $T = 0.4\text{--}1$  K. This indicates that the lifetime of the excess quasiparticles in the film Al(1) was not limited by tunneling, because the time  $\tau_T$  required for the quasiparticles to escape to the other electrodes by tunneling is independent of  $T$ . The same conclusion follows by analyzing the numerical estimates for  $\tau_T$  in our tunnel junctions, which had relatively low tunnel barrier transparencies (see Ref. 1). The experimentally measured time  $\tau$  should thus be equal to the recombination time  $\tau_R$ . The dependence  $\tau_R(T)$  found by this method for

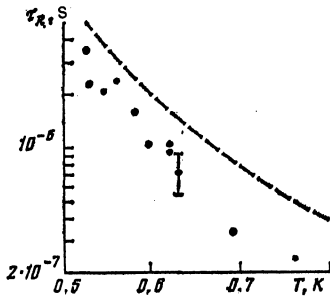


FIG. 5. Temperature dependence of the lifetime  $\tau_R$  for the film Al(1). The dashed curve shows the theoretical dependence (6) for an aluminum film with  $T_c = 2.2$  K and  $l = 7$  Å.

the film Al(1) is shown in Fig. 5. Although the current plateau on the I-V characteristic is less pronounced for specimens with larger  $(\Delta_1 - \Delta_2)/\Delta_1, \tau_R$  can still be estimated quite accurately by this technique.

The values  $\tau_R$  found for all of the specimens are satisfactorily described by Eq. (6), derived for the case  $q_{2\Delta} l \ll 1$  corresponding to the experimental conditions. In the films studied,  $l = 5-15$  Å and  $q_{2\Delta} l = 0.07-0.2$ . The dashed curve in Fig. 5 shows the theoretical dependence (6). Considering the freedom in choosing the numerical values appearing in (6), as well as the large experimental error ( $\sim 30\%$ ) in determining the mean free path of the electrons in the films, the agreement between theory<sup>6</sup> and experiment may be regarded as satisfactory. The values  $\tau_R$  are also accurately described by Eq. (5) derived for the "pure" case. [The lifetimes  $\tau_R$  calculated for the case  $q_{2\Delta} l \gg 1$ <sup>12</sup> turn out to be  $\sim 20\%$  less than  $\tau_R$  calculated by (6) for the same temperatures and  $l = 7$  Å.] This agreement, however, is a fortuitous consequence of the fact that for  $T$  fixed,  $\tau_R$  depends nonmonotonically on the parameter  $q_{2\Delta} l$ . The nonmonotonic dependence  $\tau_\epsilon(q_l)$ , discussed previously in Ref. 13, occurs because as  $q_{2\Delta} l$  decreases, the weakening of the electron-phonon interaction is offset by an abrupt enhancement of the role played by the transverse phonons, as is apparent from the factor  $1 + 3/2 \cdot (u_l u_l)^2$  in (7). We remark that the films were two-dimensional as far as phonons of energy  $\hbar\omega \approx 2\Delta_1$  were concerned ( $q_{2\Delta} a_1 < 1$ ). For this reason, the good agreement of the experimental values  $\tau_R$  with the results of the theory in Ref. 6, in which a three-dimensional phonon spectrum is considered, would appear to indicate that the phonon spectrum does not change significantly in these films, which were deposited on dielectric substrates.

The dependence  $\tau_R(T)$  can be used to calculate  $\delta N_1(I_i, T)$  for arbitrary  $I_i, T$  and to compare the experimental results with the theoretical predictions for ANR without fitting any parameters to the experimental data. We will first discuss the range of temperature and injection currents for which ANR is observed.

Condition (2) for ANR to be observable was derived in Ref. 2 under some assumptions regarding the form of the nonequilibrium distribution function for the quasiparticles (a Fermi function with effective temperature  $T$  and  $\mu \neq 0$  was assumed). Since  $\exp(\mu_i/kT) = 1 + \delta N_i/N_{iT}$  and  $\delta N_1 \gg \delta N_2$ , we can rewrite (2) as

$$\delta N_1 > N_{iT} \frac{\Delta_1}{kT} \left[ \left( \frac{\Delta_1}{\Delta_2} \right)^2 - 1 \right]. \quad (10)$$

In our experiment the quasiparticles were injected in a nar-

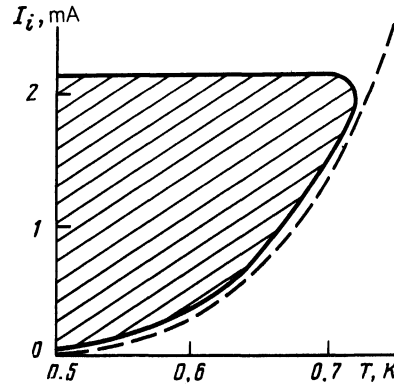


FIG. 6. Temperatures and injection currents (hatched region) for which ANR was observed in our specimen ( $V_d = 0$ ). The dashed curve gives the theoretical boundary for ANR at  $V_d = 0$  calculated by (4) and (10) with  $\tau_R(T)$  found experimentally.

row energy interval  $\delta\epsilon \ll \Delta_1$  (see insert 1 to Fig. 3); the distribution function for the quasiparticles was therefore not a Fermi distribution, because for  $T = 0.2-0.4 T_c$  the inelastic scattering and recombination times are comparable for quasiparticles with energies  $\epsilon \approx \Delta$  (Ref. 5). However, the ANR effect should not be sensitive to the specific form of the nonequilibrium distribution function. With this assumption condition (10), which is expressed in terms of an extensive parameter (the total number of excess quasiparticles), should apply more generally than the original expression (2). Figure 6 shows the region within which ANR was observed for this specimen; the region of existence was found by analyzing families of probe junction I-V characteristics (similar to the ones in Fig. 3) recorded at various temperatures. This region contained numerous experimental points, and the error in determining its boundary was less than  $\Delta I_i \approx 10 \mu\text{A}$  and  $\Delta T \approx 0.01$  K. The hatched curve shows the theoretical boundary of the region, calculated by (4) and (10) with  $\tau_R(T)$  obtained independently. Expression (10) satisfactorily describes the experimental data for  $I_i \leq 2.2$  mA; at higher injection currents (as noted above), the superconductivity of the central electrode is quenched. Good agreement of the theory in Ref. 2 with the experimental results is also observed for specimens with larger differences  $\Delta_1 - \Delta_2$ . According to Eq. (10), much higher injection currents are needed to observe ANR in these specimens (for  $\Delta_1$  and  $T$  fixed). The finding that ANR begins at  $|V_d| \approx (\Delta_1 - \Delta_2)/e$  (Fig. 3) as  $I_i$  increases also agrees with the predictions of the theory for the case  $(\Delta_1 - \Delta_2)/\Delta_1 \ll 1$ . We emphasize once again that no parameter fitting was used in the above comparison of theory and experiment.

We next discuss the shape of the I-V characteristic when ANR is present. The symmetry of the I-V characteristic relative to the coordinate origin indicates that the role of any imbalance in the populations of the branches of the quasiparticle spectrum, which in principle could arise during tunnel injection,<sup>14</sup> is in fact minimal. This is because under the experimental conditions the quasiparticles were injected in a narrow range of energies  $\epsilon - \Delta \ll \Delta$ , and the recombination time of the excess quasiparticles was also considerably longer than the relaxation time  $\tau_Q$  for the population imbalance. [For our Al films at  $T \leq 1$  K we find that  $\tau_Q < \tau_R(T)$  even if we ignore all but one of the possible imbalance relaxation mechanisms—namely, impurity scattering in a system

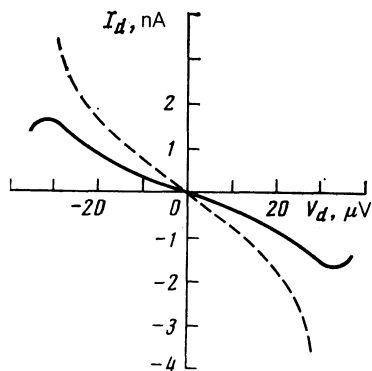


FIG. 7. Current-voltage characteristic for the probe tunnel junction recorded at  $T = 0.52$  K and  $I_i = 0.2$  mA (solid curve). The dashed curve shows the I-V characteristic calculated by (1) for the same values of  $T$  and  $I_i$ . (The theoretical dependence  $I_d(V_d)$  has extrema at  $|V_d| = (\Delta_1 - \Delta_2)/e \approx 40$   $\mu$ V.)

with an anisotropic energy gap<sup>14</sup>.] The experimental data may thus be compared with the results in Ref. 2, in which the effects of population imbalance were not considered. Along with the experimental I-V characteristic, Fig. 7 shows the theoretical curve calculated by (1) and (4) using the lifetime  $\tau_R(T)$  found at  $T = 0.52$  K. Expression (1) ignores the experimentally observed broadening of the extrema on the I-V characteristic at  $|V_d| = (\Delta_1 - \Delta_2)/e$  caused by the spatial variation of the order parameter over the surface of the probe tunnel junction, by external noise, and other factors. The discrepancy between theory and experiment is therefore greatest in the immediate vicinity of  $|V_d| = (\Delta_1 - \Delta_2)/e$ . For  $|V_d| < (\Delta_1 - \Delta_2)/e$  these factors have little effect on the shape of the I-V characteristic, and the experimental curves  $V_d(I_d)$  are satisfactorily described by the theory<sup>2</sup> for all the temperatures and injection currents investigated. The quantitative discrepancy, which never exceeds a factor of two or three, is presumably due to errors in finding  $\tau_r$  and the various other parameters appearing in (1). The differential conductivity  $G_0$  of the probe junction at zero bias voltage is least sensitive to the effects of the factors broadening the extrema on the I-V characteristics. Figure 8 shows the experimental and theoretical curves  $G_0(I_i)$  for  $T = 0.52$  K. The theoretical expression

$$G_0 = \Delta_2^2 N_{1T} \left\{ \frac{\Delta_1}{kT} \left[ \left( \frac{\Delta_1}{\Delta_2} \right)^2 - 1 \right] - \frac{\delta N_1}{N_{1T}} \right\} / 2N(0)R_N(\Delta_1^2 - \Delta_2^2)^{3/2} \quad (11)$$

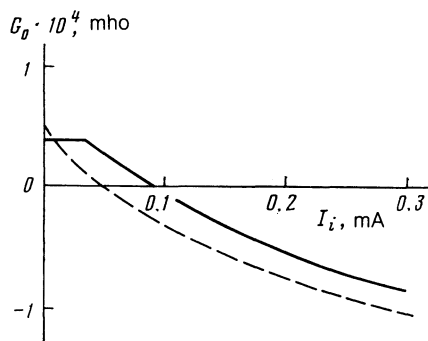


FIG. 8. Differential conductivity  $G_0$  of the probe junction ( $V_d = 0$ ) at  $T = 0.52$  K as a function of  $I_i$  (solid curve). The horizontal section corresponds to flow of supercurrent through the injecting junction. The dashed curve shows the theoretical dependence  $G_0(I_i)$  calculated by (11).

for the tunnel conductivity gives a reasonably close approximation of the experimental curves  $G_0(I_i)$  for all of the specimens investigated. The experimental and theoretical curves  $G_0(I_i)$  in Fig. 8 diverge for small  $I_i$ , because the injecting tunnel junction for this specimen was a Josephson junction with critical current  $I_c = 0.035$  mA. At low temperatures  $T \approx 0.5$  K,  $|G_0(I_i)|$  is observed to increase as far as  $I_i \approx 1$  mA, beyond which heating becomes important (see Fig. 4). When  $I_i$  increases further to the critical current for the film Al(1)  $|G_0|$  remains essentially constant, and for injection currents in this range the divergence between the experimental and theoretical curves  $G_0(I_i)$  becomes considerable. We note that for  $|V_d| < (\Delta_1 - \Delta_2)/e$ , the form of the I-V characteristic (and hence also  $G_0$ ) ceases to depend on temperature at sufficiently high currents. Under these conditions  $G_0$  depends only on the excess quasiparticle concentration  $\delta N_1$ , which is much greater than the equilibrium quasiparticle concentration  $N_{1T}$ .

## 5. CONCLUSIONS

The tunnel injection used to create the excess quasiparticle concentration in our experiment has definite advantages over optical excitation, at least as far as the investigation of the basic properties of absolute negative resistance is concerned. Of particular importance for quantitative comparisons with theory is the fact that the number of injected quasiparticles is known precisely. However, ANR should also be observable when the excess quasiparticles are generated by photons, phonons, or other particles, and this fact can be exploited to design new types of particle detectors that employ superconducting tunnel junctions (see, e.g., Ref. 15 and the references therein). In this case the thickness of the electrode with the larger  $\Delta$  must be greater than the mean free path of the particles being detected. (The choice of an ultrathin central electrode in our experiment is appropriate for injection: at a fixed injection current, the excess quasiparticle concentration increases as the electrode is made thinner. (We remark that regardless of the method of excitation, ANR is more easily achieved if the energy gap difference  $\Delta_1 - \Delta_2$  is small. The large values  $(\Delta_1 - \Delta_2)/\Delta_1 \sim 1$  used in Refs. 16 and 17 were apparently the main reason why ANR was not observed (those experiments investigated the change in the I-V characteristics for Pb-Sn and PnBi-Al tunnel junctions when the electrode with the larger  $\Delta$  was illuminated by light.) The choice of electrode material in the tunnel junction also plays a role, since ANR is more easily observed if superconductors with low state densities  $N(0)$  are employed. Finally, low temperatures ( $\Delta/kT \gg 1$ ), for which the excess quasiparticles have a relatively long lifetime, are essential if ANR is to occur. The above conditions are also important if one is to observe instability in Josephson tunnel junctions during injection of excess quasiparticles into the electrode with the larger  $\Delta$  (Ref. 18).

In summary, we conclude that the results of the above experiments on absolute negative resistance in superconducting tunnel junctions are adequately described by the theory in Ref. 2, and the ANR condition (10), expressed in terms of the excess quasiparticle concentration, holds for a wider class of nonequilibrium distribution functions than has hitherto been assumed. The ANR effect should clearly be of interest in practical applications as well as in further

studies of nonequilibrium superconductivity.

We are grateful to A. G. Aronov, M. Yu. Reizer, A. V. Sergeev, and B. Z. Spivak for helpful discussions.

<sup>11</sup>At  $T = 0.5$  K the thermal resistance of the Al-film/glass substrate (immersed in liquid  $^3\text{He}$ ) is  $\sim 10^3 \text{ cm}^2 \cdot \text{K}/\text{W}$  (Ref. 10), and the temperature difference between a specimen of area  $1 \text{ mm}^2$  and the thermostat may exceed  $0.1$  K for  $V_i \approx (\Delta_1 + \Delta_2)/e \approx 0.5$  mV and  $I_i = 1$  mA.

<sup>12</sup>The value  $4.4 \cdot 10^{-7}$  s for  $\tau_0$  ( $\sim T_c^{-3}$ ) given in Ref. 5 at  $T_c = 1.19$  K can be used to get the estimate  $\approx 7 \cdot 10^{-8}$  s for  $\tau_0$  at  $T_c = 2.2$  K.

<sup>1</sup>K. Cray, in: *Nonequilibrium Superconductivity, Phonons and Kapitza Boundaries* (Plenum Press, New York 1981), p. 131.

<sup>2</sup>A. G. Aronov and B. Z. Spivak, *Pis'ma Zh. Eksp. Teor. Fiz.* **22**, 218 (1975) [*JETP Lett.* **22**, 101 (1975)].

<sup>3</sup>M. E. Gershenzon and M. I. Falei, *Pis'ma Zh. Eksp. Teor. Fiz.* **44**, 529 (1986) [*JETP Lett.* **44**, 682 (1986)].

<sup>4</sup>A. Rothwarf and B. N. Taylor, *Phys. Rev. Lett.* **19**, 27 (1967).

<sup>5</sup>S. B. Kaplan, C. C. Chi, D. N. Langenberg, *et al.*, *Phys. Rev. B* **14**, 4854 (1976).

<sup>6</sup>M. Yu. Reizer and A. V. Sergeev, *Zh. Eksp. Teor. Fiz.* **90**, 1056 (1986) [*Sov. Phys. JETP* **63**, 616 (1986)].

<sup>7</sup>R. C. Dynes and J. P. Garno, *Phys. Rev. Lett.* **46**, 137 (1981).

<sup>8</sup>L. Solymar, *Superconductive Tunneling and Applications* (Chapman and Hall, London, 1972).

<sup>9</sup>V. P. Andratskiĭ, L. M. Grundel', V. N. Gubankov, and N. B. Pavlov, *Zh. Eksp. Teor. Fiz.* **65**, 1591 (1973) [*Sov. Phys. JETP* **38**, 794 (1973)].

<sup>10</sup>A. C. Anderson, in: *Nonequilibrium Superconductivity, Phonons and Kapitza Boundaries* (Plenum Press, New York, 1981), p. 1.

<sup>11</sup>K. E. Gray, *J. Phys.* **1**, 290 (1971).

<sup>12</sup>S. B. Kaplan, *J. Low Temp. Phys.* **37**, 343 (1979).

<sup>13</sup>A. Schmid, in: *Localization, Interaction and Transport Phenomena* (Springer Verlag, New York, 1985), p. 212.

<sup>14</sup>C. C. Chi and J. Clarke, *Phys. Rev. B* **19**, 4495 (1979).

<sup>15</sup>N. E. Booth, *Appl. Phys. Lett.* **50**, 293 (1987).

<sup>16</sup>Yu. M. Gerbshtein, E. I. Nikulin, and B. Z. Spivak, *Fiz. Tverd. Tela* **20**, 1067 (1978) [*Sov. Phys. Solid State* **20**, 616 (1978)].

<sup>17</sup>A. D. Smith, W. J. Skocpol, and M. Tinkham, *Phys. Rev. B* **21**, 3879 (1980).

<sup>18</sup>A. I. Larkin and Yu. N. Ovchinnikov, *Pis'ma Zh. Eksp. Teor. Fiz.* **39**, 556 (1984) [*JETP Lett.* **39**, 681 (1984)].

Translated by A. Mason